

Investigation of Factors that Affect Site Selection for Geothermal Energy Extraction in North Dakota

Ogonna Obinwa Author

715 P Street, Sacramento, CA 95814

Ogonna.obinwa@conservation.ca.gov

Keywords: geothermal, direct use, heat, low temperature, power generation, resource estimate, aquifer, porosity, permeability

ABSTRACT

Geothermal energy is independent renewable energy extracted from deep and shallow subsurface to provide electricity and heat for many applications. At shallow depths of about 3000 feet (914 meters), temperatures as high as 70°C could be extracted and used for domestic and commercial heating systems. Deeper and hotter resources are usually available at depths greater than 10000 feet (3048 meters). The hotter the extracted fluid temperature, the better it is suited for electricity generation. New technologies such as binary cycle systems have made it possible to use moderately hot liquids for electricity generation. However, specific conditions must be in place for a geothermal reservoir's existence and economical heat extraction. This study investigates these conditions to help determine geothermal site selection in North Dakota. There are many oil and gas wells in North Dakota, mainly spread across the Williston Basin. Data from some of these wells were used to obtain valuable information for this research study. Some of the wells are in the abandoned status. The abandoned wells, in most situations, have lost their economic value for producing oil and gas. However, they could be good candidates to use geothermal resources. The geothermal energy system has faced many challenges since its inception. Some of the biggest challenges are the cost of extracting the energy for use and scalability. Since natural sources of great geothermal energy sources are geographically limited, an efficient method to determine site selection for geothermal extraction becomes imperative.

1. INTRODUCTION

1.1 General

The heat energy generated from the ground can be used for various purposes such as electricity, direct heating of homes, spas, and mineral baths. As the demand for electricity generation from geothermal energy continues to grow worldwide (Bertani, 2016), the energy industry faces the challenge of reducing drilling costs to confirm geothermal resources' existence. This research work aims at investigating several factors that are critical in determining a high-grade geothermal resource. These factors include the temperature distribution and the rock's specific heat; the total and the effective porosity; the permeability; sufficient fluid in place; reservoir thickness; and an adequate reservoir recharge of fluids (Muffler & Cataldi, 1977). Other properties necessary for an economic geothermal energy extraction include adequate production capacity and water chemistry (Gosnold, 1991). This research study investigates some of these factors. It demonstrates how the process could be applied in geothermal energy site selection in North Dakota.

1.2 Purpose and Scope

This research work is directed towards assessing factors critical in determining sites for geothermal extraction in North Dakota. In this research work, records of temporarily abandoned wells located in the North Dakota Industrial Commission (NDIC) database were used. The purpose of considering the temporarily abandoned wells is to evaluate the possibility of repurposing the wells for geothermal energy extraction and, at the same time, provide information on possible nearby new drills. Geothermal energy extraction projects have faced setbacks because of the cost of drilling new wells. Hence, cost-saving operations that will reuse wells designated for plugging and abandonment will be invaluable. Using the existing well data also provides a clear picture of different formations at varying depths. It helps evaluate the factors critical in determining geothermal resource location and provides some certainty in forecasting thermal energy production.

1.3 Method of Study

This project aims to leverage existing infrastructures by investigating the potential of converting wells on temporarily abandoned status to geothermal wells. The project's sources include oil and gas wells data from the North Dakota industry Commission (NDIC) website. Data from selected wells will be used to create a regional heat map for temperature-depth estimation. The corrected temperatures at depth are calculated using Thermostratigraphic (TSRAT) estimation (Gosnold et al., 2012). The geothermal gradient is calculated for the areas identified with geothermal resource potentials. Mapping tools such as Surfer and ArcGis will be used in the evaluation of the site selection locations. Stratigraphic and thermal conductivity data will be used to analyze the temperature at depth. Finally, North Dakota Stratigraphic Column map will be used to evaluate target resource formation properties. The completion formation is determined using the North Dakota Stratigraphic column (Murphy et al., 2009).

2. LITERATURE REVIEW

The earth's interior reaches a temperature greater than 4000°C, and this geothermal energy flows continuously to the surface (Green & Nix, 2006). While much of the earth's energy cannot be recovered, a small percentage recovered has shown that geothermal energy can play an essential role in the energy supply (Liu et al., 2021). Such countries are Iceland (27% of power) and El Salvador (26% of power) (Falcone et al., 2018). The International Energy Agency Energy Market Report 2013 announced that by 2050, geothermal generation could reach 1400 TWh per year, around 3.5% of global electricity production, and contribute 5.8 EJ in geothermal heating (Medium-Term Renewable Energy Market Report 2013, 2013). In addition, many countries explore ways to be less dependent on energy imports. Thus, the need to harness the energy from the earth's subsurface continues to grow (Falcone et al., 2018).

2.1 Temperature Estimation

Geothermal energy as an abundant renewable energy source is considered constant and independent (Falcone et al., 2018). There are three classes of geothermal energy sources: high temperature (> 150°C), medium-temperature (90-150°C), and low-temperature source (< 90°C) (Nian & Cheng, 2018). In North Dakota, strata-bound geothermal resource temperature ranges from less than 90°C to an intermediate temperature between 90°C and 150°C (Gosnold, 1991). Depending on the geothermal sources' temperature, the produced fluid can be used for heating, cooling, and power generation; depth, however, is necessary for power generation (Falcone et al., 2018). Deep sedimentary basins underlie one-half of North Dakota, and there is significant potential for the occurrence of geothermal resources. The deep sedimentary basins are capped with thick low thermal-conductivity shale and are underlain by four major aquifers (Gosnold, 1991). Heat is not the only factor necessary for the determination of geothermal site selection. Several factors contribute to the determination of whether a geothermal resource can be extracted economically. These factors include adequate temperature, adequate production capacity, favorable water chemistry, fluid pressure, permeability, and the aquifer's thickness (Gosnold, 1991). Subsurface temperatures vary significantly throughout North Dakota according to variations in thermal conductivities within the sedimentary strata. However, the formations within the basins remain continuous (Gosnold, 1991).

Since the formations remain continuous within the basins, Gosnold, 1991, suggested that thermal conductivities measured on samples from a few sites might be applied to the lithologic units throughout the region using the following mathematical relation:

$$T(z) = T_0 + \sum_{i=1}^n \frac{QZ_i}{\lambda_i} \quad (1)$$

T_0 is surface temperature, Q is heat flow, Z_i is the thickness of the i th stratum, and λ_i is the thermal conductivity of the i th stratum (Gosnold, 1991). Thus, the subsurface temperature is determined by the local heat flow, known from the boreholes' direct temperature measurements, the mean average surface temperature, the thermal conductivities, and the thickness of strata (Gosnold, 1991).

2.2 Porosity and Permeability

The porosity and permeability of several formations were obtained from the research work conducted by Smith et al., 2017. In their work, the porosity was tested using a Helium Porosimeter and Boyles Law calculation was applied to determine the grain volume of each sample (Smith et al., 2017). Then, this value is subtracted from the predetermined bulk volume to determine the amount of void space (porosity) in the rock (Smith et al., 2017). Table 1. Shows results of the tested samples for relative permeability. Table 2 shows the porosity and permeability data collected for each of the samples tested.

Table 1 - Seven Samples tested for relative permeability (Smith et al., 2017)

	Clastic			Carbonate			
NDIC Well	165	658	17467	13718	13718	16409-P	16409-P
Formation	Inyan Kara	Broom Creek	Deadwood/ Black Island	Lodgepole	Lodgepole	Mission Canyon	Mission Canyon
Sample depth, m	1510.9	2343.3	2885.0	3007.9	3005.4	1893.3	1899.8
Sample ID	120720	121185	120743	120729	120726	120735	120740
Quartz	73.3	87.8	93.2	Trace	0.6	4.8	0.5
Calcite				91.0	68.8	20.7	91.5
Dolomite		3.2		1.4	22.0	46.7	1.6
Ankerite					2.7	17.3	
Plagioclase	7.1	3.1	0.8			0.4	
K-Feldspar	3.7	4.0	1.5	1.4	1.1	2.4	1.6
Anatase				0.5			
Hematite	0.3			0.3	0.3	0.6	
Halite	0.3	1.5		0.8	Trace	1.0	0.4
Anhydrite		0.5					
Sylvite				Trace	Trace	0.5	
Pyrite	Trace					Trace	
Kaolinite	4.0		Trace	2.2	1.0		1.0
Illite	4.9		1.7		0.6	2.0	0.8
Chlorite	6.1		2.6	2.0	2.5	3.4	2.6

Although porosity-permeability relationships are not well known in shales, the Kozeny -Carman relationship relates permeability and porosity in sedimentary formations as follows:

$$K=20\phi^5/S_0 \quad 2(1-\phi)^2 \quad K=20\phi^5/S_0 \quad 2(1-\phi)^2 \quad (1)$$

where K is permeability (in m^2), ϕ' is the porosity corrected for one molecular layer adsorbed water, and S_0 is the specific surface area (in m^2/m^3) (Jean Burrus (2), Kirk Osadetz (3), 1996).

Table 2 - Porosity and permeability of collected samples (Smith et al., 2017)

Sample no.	Depth, m	Formation	L, cm	D, cm	BV, ¹ cm^3	GD, ² g/cm^3	PV, ³ cm^3	ϕ , %	K_{air} , mD
120720	1510.9	Inyan Kara	3.9	3.0	27.7	2.6	5.9	21.5	95.2
121185	2343.3	Broom Creek	3.3	3.0	22.4	2.6	5.7	25.5	850
120743	2885.0	Deadwood/BI	5.7	3.0	40.6	2.6	6.4	15.8	481
120729	3007.9	Lodgepole	5.9	3.0	41.6	2.7	5.7	13.6	29.7
120726	3005.4	Lodgepole	2.4	3.0	17.4	2.7	1.0	5.7	0.117
120735	1893.3	Mission Canyon	2.5	3.0	17.5	2.8	3.1	17.9	0.253
120740	1899.8	Mission Canyon	2.3	3.0	16.0	2.7	1.6	9.8	0.31

Table 3 - Porosity and permeability of some North Dakota formations

Formation	Porosity (%)	Permeability (mD)	Source
Inyan Kara Fm	20-30	10 - 100	"(Bader, 2017)"
Spearfish Fm	12-15	<0.1 - 320	"(LeFever, 2011)"
Broom Creek Fm	25.5 (average)	Can be up to 850	"(Smith et al., 2017)"
Lodgepole Fm	13.6 (average)	29.7 (average)	"(Smith et al., 2017)"
Red River Fm	10-24	<1 - 62.8	"(Hartig, 2018)"
Deadwood Fm	15.8 (average)	Can be up to 481	"(Smith et al., 2017)"

2.3 Aquifers

Williston Basin underlies western North Dakota, northwestern South Dakota, eastern Montana, southern Manitoba, and southeastern Saskatchewan (Majorowicz et al., 1988). There are at least twelve regional aquifers in the Williston Basin (Gosnold, 1991). At least four of these aquifers underly North Dakota, and these aquifers include Inyan Kara, Madison, Duperow, and Red River (Gosnold, 1991).

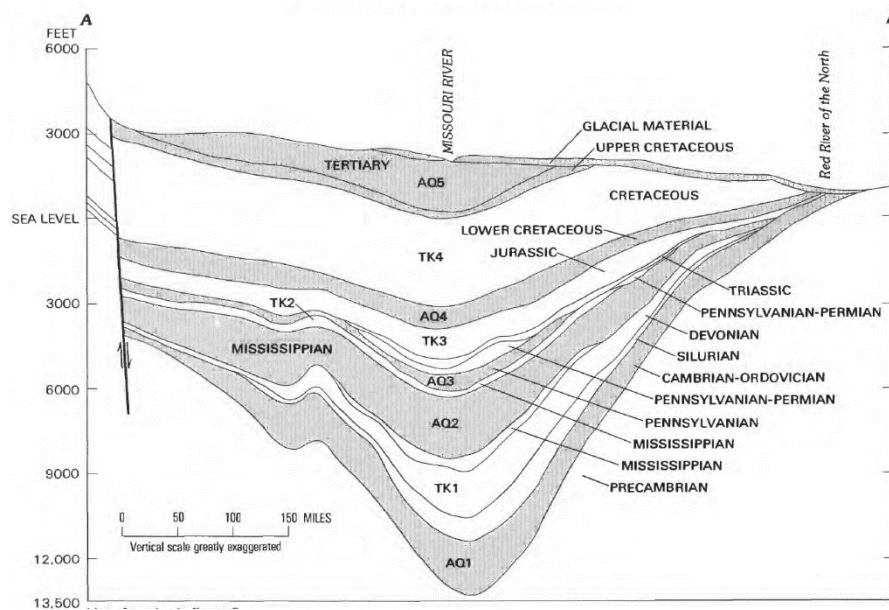


Figure 1 - Cross-sectional diagram of aquifers across east-west of North Dakota (modified from Downey & Dinwiddie, 1988)

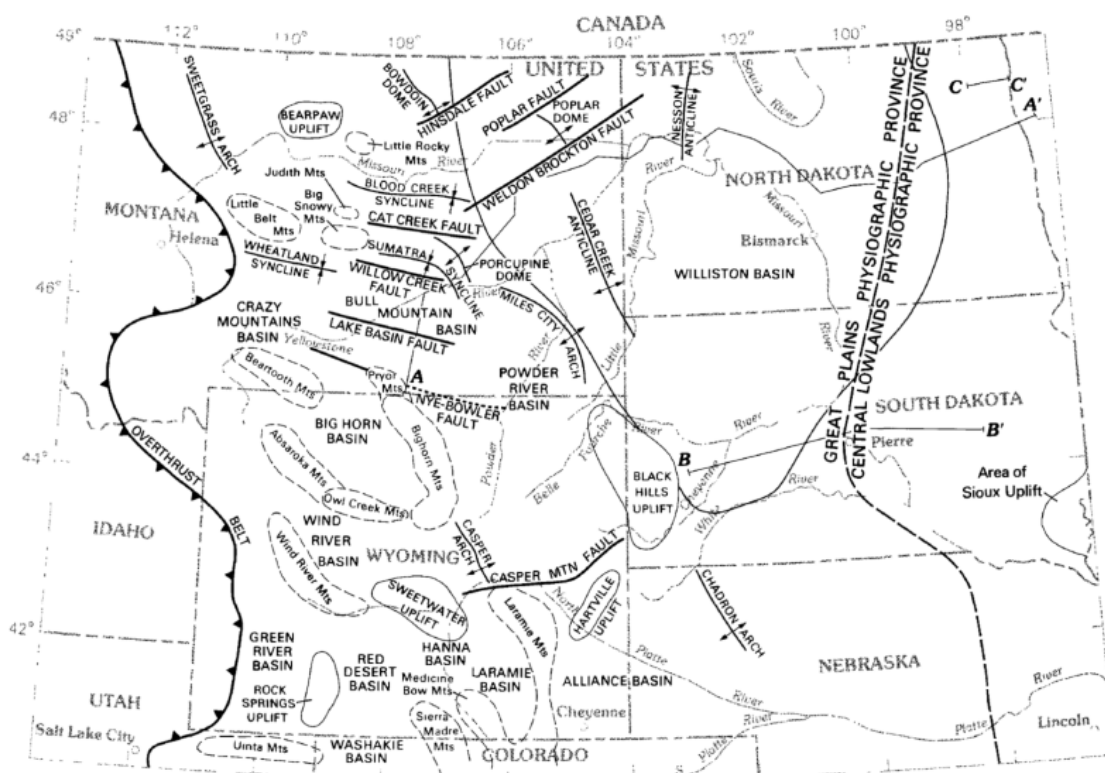


Figure 2- Map showing A-A' used in creating fig.1 (modified from Downey & Dinwiddie, 1988)

Table 4 - Stratigraphic column showing depth, thickness, and the lithology of the formations (Murphy et al., 2009)

2.4 Stratigraphy and Formation Thickness

The North Dakota Geological Survey provides a stratigraphic column detailed as shown in Table 4. The table contains information about age, the average thickness of formation, the lithology, and potential resources available in each formation. Figure 3 shows stratigraphy and sedimentary facies of the madison limestone with additional details on porosity.

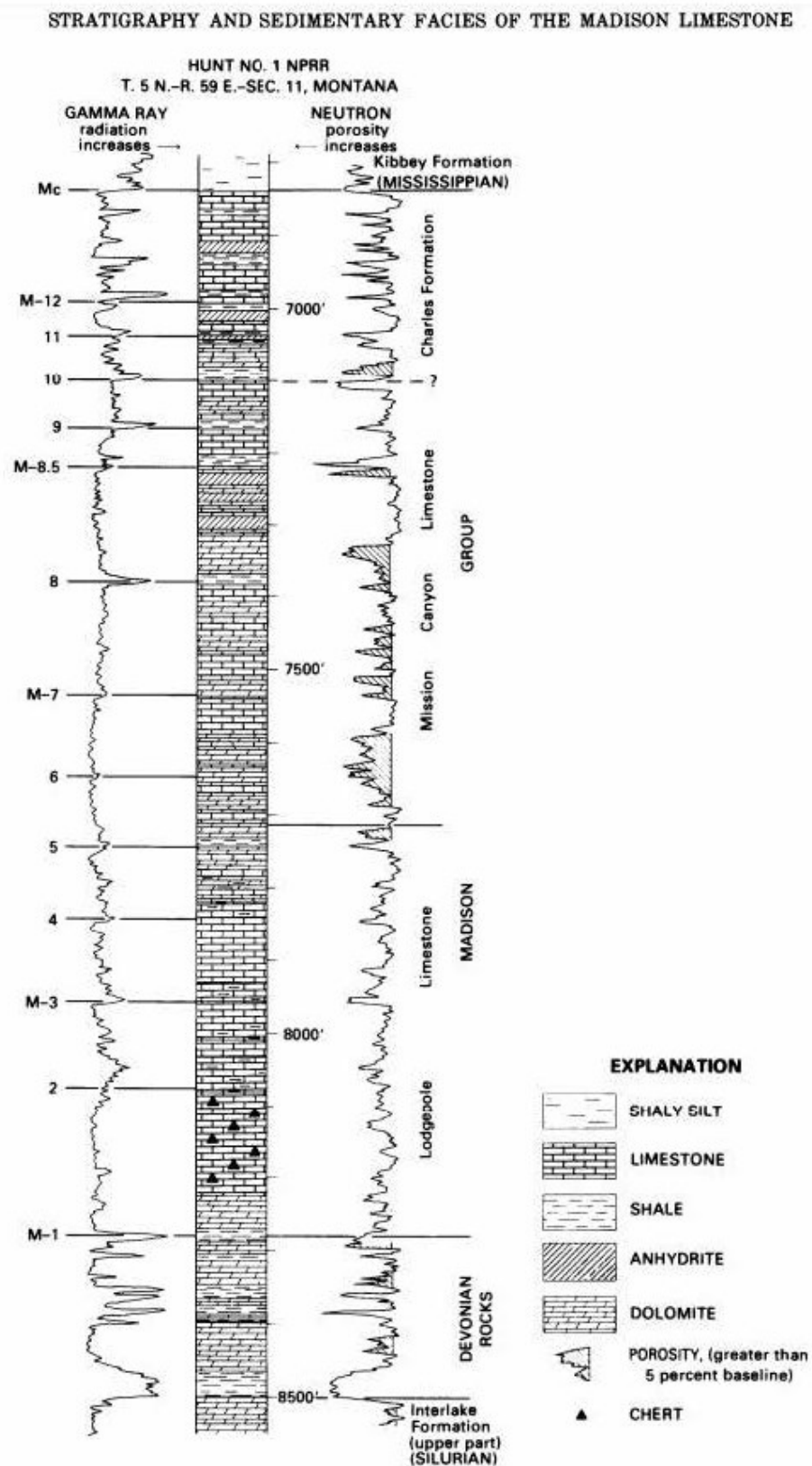


Figure 3- Stratigraphy and Sedimentary Facies of the Madison Limestone (Peterson, 1984)

3. METHODOLOGY

3.1 Process Flow Chart

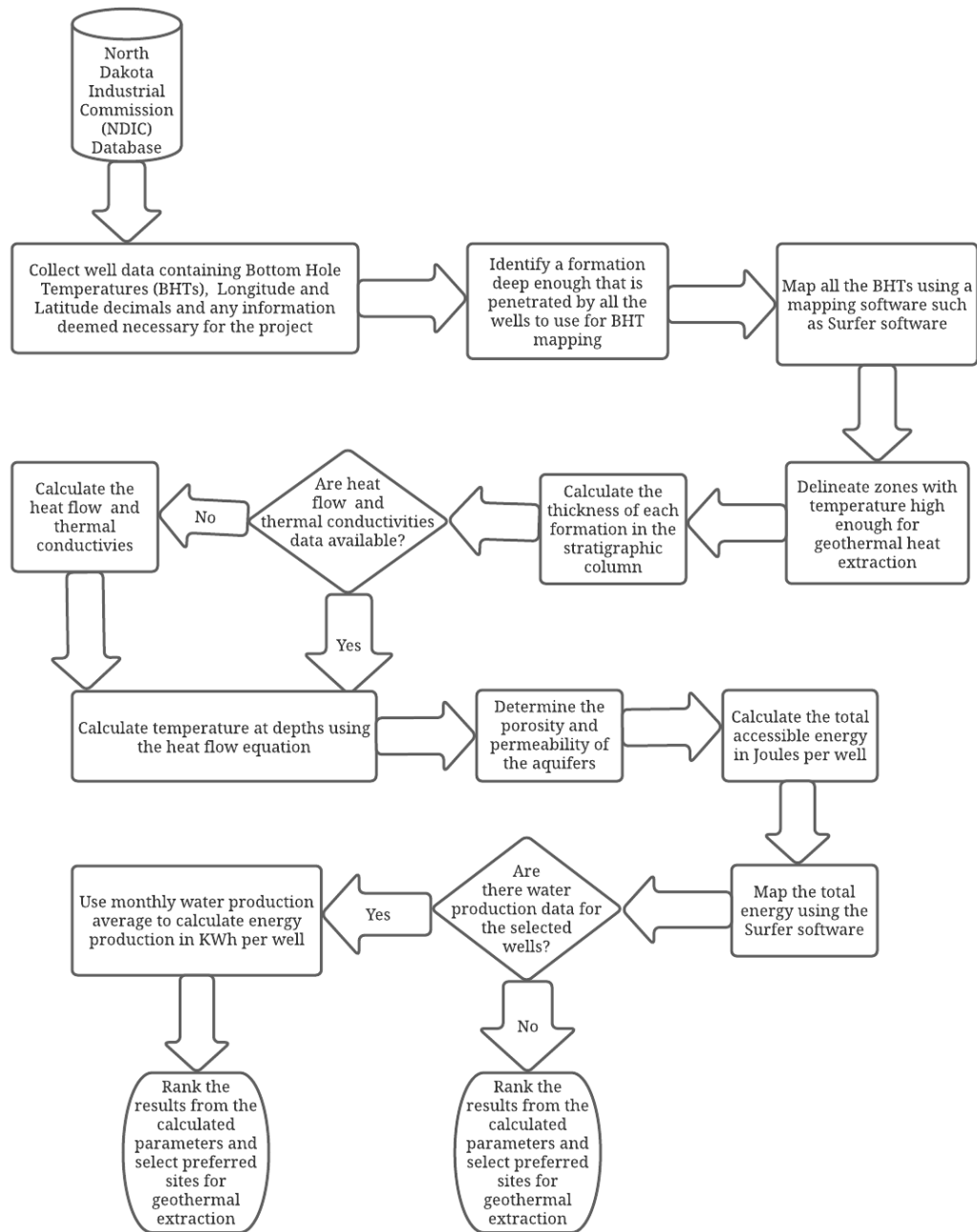


Figure 4 - A flow chart showing steps followed to complete the study

3.2 Data Collection and Creation of Heat Map

In this research study, oil and gas wells data were collected from the North Dakota Industrial Commission (NDIC) website. Madison formation is selected to be used in creating the heat map of North Dakota. The reason is that the top of the Madison formation, on average, is over 2000 meters (6562 feet) deep, and most oil and gas wells go through it. The input data in the Surfer software include the bottom hole temperatures of the wells and the well locations. The resulting map provides an estimated visual of geothermal heat source areas.

The findings from the map indicate higher temperatures in the west of North Dakota. A focused study was conducted on the western part of North Dakota to calculate the temperature at a depth of every formation. Further sorting of the wells was done to select vertical wells that penetrate the Red River formation. Vertical wells are considered in this study because it helps calculate a more accurate temperature gradient (Beardsmore & Cull, 2001). Red River formation is chosen because it is the deepest of the four major aquifers in North Dakota (Gosnold, 1991). The four major aquifers in North Dakota are Inyan Kara, Madison, Duperow, and Red River (Gosnold, 1991). Figure 1 shows that the Cambrian-Ordovician system, which is the location of the Red River aquifer.

3.3 Calculation of Temperature at Depth Using Fourier's Equation of Heat Flow

A total of 28 wells were identified for further analysis. First, the depths of the top of the formations of the wells were obtained from the NDIC database. Then, the thickness of each formation identified in the location of the wells was calculated. The difference of the tops gives the thickness. Figure 6 shows the locations of the selected wells.

The heat flow for North Dakota has been determined (Gosnold & Njoku, 2017). However, the bottom hole temperatures do not reflect the actual temperatures at depth. Therefore, the linear relationship in Fourier's law is used

$$q = \lambda(dT/dz) \quad (2)$$

where q is the heat flow in mWm^{-2} , λ is the thermal conductivity in $\text{Wm}^{-1}\text{K}^{-1}$, and dT/dz is the temperature gradient and was used to calculate the temperatures at depths (Gosnold & Njoku, 2017). The heat flow value used in this study is 60 mWm^{-2} .

The actual temperatures at depth were calculated using the following relation:

$$T(z) = T_0 + \sum_{i=1}^n \frac{QZ_i}{\lambda_i} \quad (3)$$

Where T_0 is surface temperature, Q is heat flow, Z_i is the thickness of the i th stratum, and λ_i is the thermal conductivity of the i th stratum (Gosnold, 1991).

3.4 Calculation of the Accessible Resource Base

The accessible resource base is a function of the volume of fluid that can be produced and the temperature of the aquifer. The accessible resource base was calculated using the following equation:

$$Q = (\rho c)_f A D (T - T_{ref}) \quad (4)$$

Where Q is the accessible resource base, $(\rho c)_f$ is the volumetric specific heat of the aquifer, A is the reservoir area, D is the reservoir thickness, T is the reservoir temperature, T_{ref} is the reference temperature (15°C) (Sorey et al., 1970). The volume of the aquifer was calculated as the thickness of the aquifer and the area of the aquifer. It was assumed that the mean area of an aquifer in North Dakota is $128,000 \text{ km}^2$ for the carbonate rocks of the Madison aquifer and $57,000 \text{ km}^2$ for the sandstone of the Dakota aquifer (Sorey et al., 1970). The volumetric specific heat of rocks found in low-temperature geothermal systems has a weighted average value of $2.6 \text{ J/cm}^3 \text{ }^\circ\text{C}$ (Sorey et al., 1970). The resource estimate was calculated by multiplying the recovery factor of 0.25 by the mean accessible resource (Sorey et al., 1970).

3.5 Power Generation Calculation for Geothermal Resources

Power generation potential was calculated using the following equation:

$$E = \rho C_v V \Delta T \quad (5)$$

Where E is the power generated, ρ is the density of water, C_v is the heat capacity of water, V is the volume of water, and ΔT is the temperature change (Gosnold et al., 2019). In this study, an average of six months of water production was used for each well. The volume was converted from bbl/day to m^3/hr . ΔT is the temperature of the reservoir minus the temperature reference. A temperature reference of 15°C is used for the entire United States (Sorey et al., 1970). Fluid temperatures at the wellhead were assumed to equal the corresponding reservoir temperatures. However, insignificant loss of heat may not be achieved in many cases. These heat losses through conduction, convection, and radiation en route to the surface need to be considered in equation (6) to get the accurate power generation from each well.

Permeability of the reservoir is an important factor considered in the power generation calculation. Permeability is a parameter that determines the volume of fluid per unit time, as shown in the integral form of Darcy's law:

$$Q = (K A / \mu L) \Delta P \quad (6)$$

Where Q is the volume per unit time, K is the permeability, A is the cross-sectional area of the reservoir, ΔP is the pressure drop, μ is the dynamic viscosity, and L is the length of the reservoir. The 6-month average volume (bbl/month) for each well was calculated using the

production data from the NDIC. Based on the relationship of volume per unit time to permeability in Darcy's equation, it means that the permeability of a reservoir plays a part in determining the power generation from the reservoir.

4. RESULTS

4.1 The Heat Map

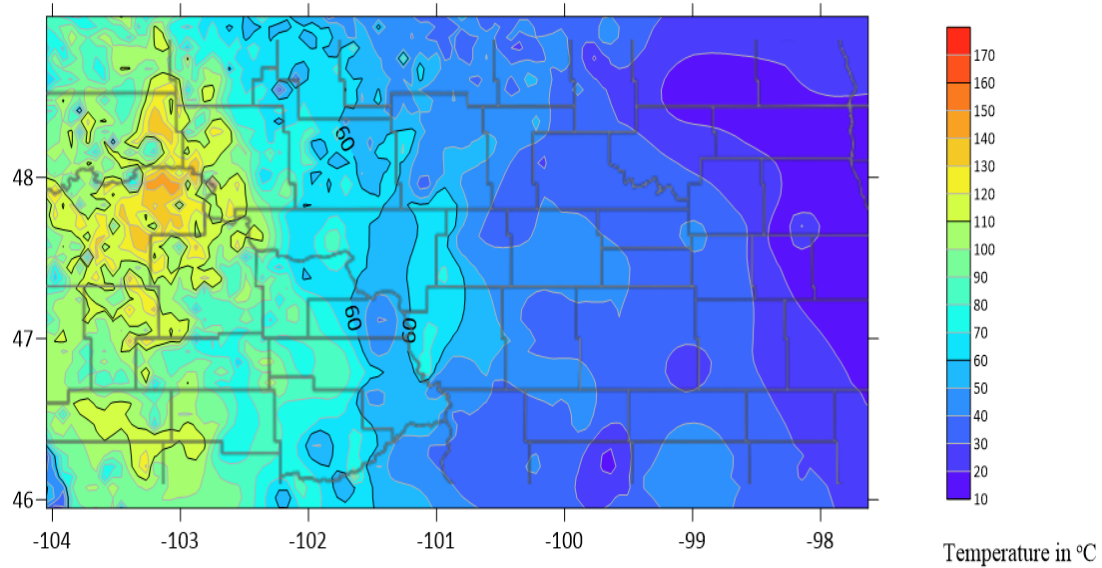


Figure 5 - Heat map of North Dakota created using the Surfer software

Figure 5 shows the heat map created using the bottom hole temperature (BHT) values. The data used in making this map were all the oil and gas wells available in the North Dakota Industrial Commission's database at the time of this study.

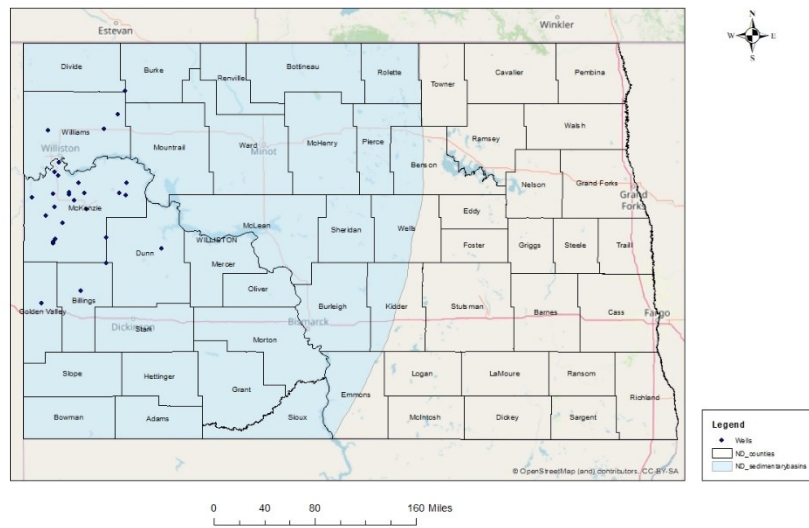


Figure 6 - Selected wells used for the study

Twenty-eight vertical wells were selected for further evaluation. Figure 6 shows the location of the selected wells. This selection was based on the preliminary results from the heat map, and the wells were selected from the area showing higher BHT in western North Dakota.

4.2 Formation Thickness Calculation

The formation thickness was calculated by subtracting the depth of each formation top from the underlying formation top. Table 5 shows the calculated thickness of all the twenty-eight wells selected for resource assessment evaluation. The thermal gradient was calculated using an average surface temperature of 4.45°C.

Table 5 – Calculated thickness of formations and temperature gradients

File Number	Top of Formation (ft)	Top of Formation (m)	Thickness (ft)	Gradient (°C/km)
9397	13166	2864	680	38.5
8945	13670	2726	330	39.3
18339	13858	5590	662	38.2
15569	13286	4745	348	40.1
11549	13177	3520	348	39.1
12378	12911	3773	338	39.9
9539	13736	2907	311	38.0
15785	14133	4811	332	39.2
9481	13430	2890	320	39.6
15669	13996	4776	324	38.9
15046	13512	4586	338	39.0
15170	13330	4624	300	39.4
7631	13816	2326	570	39.0
16330	13417	4977	303	39.8
7167	13309	2185	341	40.3
16062	14043	4896	595	38.9
6839	12737	2085	363	39.7
22750	12030	6934	570	40.4
12062	12260	3676	300	39.5
11747	13451	3580	399	39.6
16273	13294	4960	321	38.2
12173	13696	3710	339	38.1
12240	12797	3731	416	39.3
12249	12936	3733	387	39.6
11405	12613	3476	327	39.1
9300	13597	2835	364	39.2
17339	13901	5285	350	38.7
15516	12492	4729	328	39.0

4.3 Temperature Gradient Calculation

The gradient is calculated using an average of 4.45°C (Gosnold, 2021) as the surface temperature in North Dakota. Table 5 shows the calculated gradients for the twenty-eight wells. Figure 7 shows the mapped gradient by location using the Surfer software.

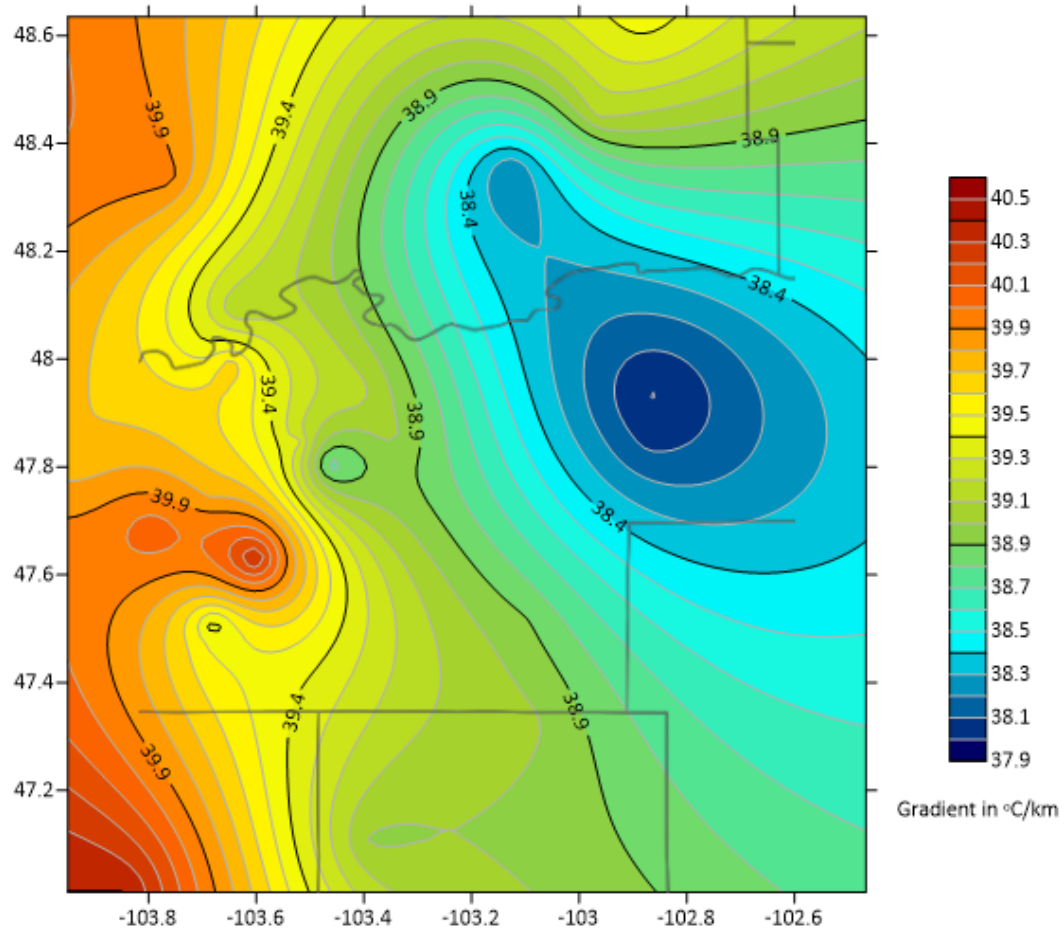


Figure 7 - Map showing temperature gradients

4.4 The Accessible Resource Base Calculation

The accessible resource base was calculated using the following equation:

$$Q = (\rho c)_f AD(T - 15^\circ\text{C}) \quad (7)$$

Where Q is the accessible resource base, $(\rho c)_f$ is the volumetric specific heat of the aquifer, A is the reservoir area, D is the reservoir thickness, T is the reservoir temperature, T_{ref} is the reference temperature (15°C) for the entire United States (Sorey et al., 1970). It was assumed that the mean area of an aquifer in North Dakota is $128,000 \text{ km}^2$ for the carbonate rocks of the Madison aquifer and $57,000 \text{ km}^2$ for the sandstone of the Dakota aquifer (Sorey et al., 1970). The calculation of the mean accessible resource, Q , was done as follows:

$$Q \text{ in Joules} = [2.6 \times 10^6 \text{ J/m}^3 \text{ }^\circ\text{C}] \times \text{Area } \text{m}^2 \times \text{Thickness (m)} \times (T_{\text{reservoir}} - 15) \text{ }^\circ\text{C} \quad (8)$$

The recovery factor of 0.25 was multiplied by the mean accessible resource to obtain the resource estimate. Thus, the resource estimate (Sorey et al., 1970), was calculated as follows:

$$\text{Resource Estimate} = 0.25 \times Q \quad (9)$$

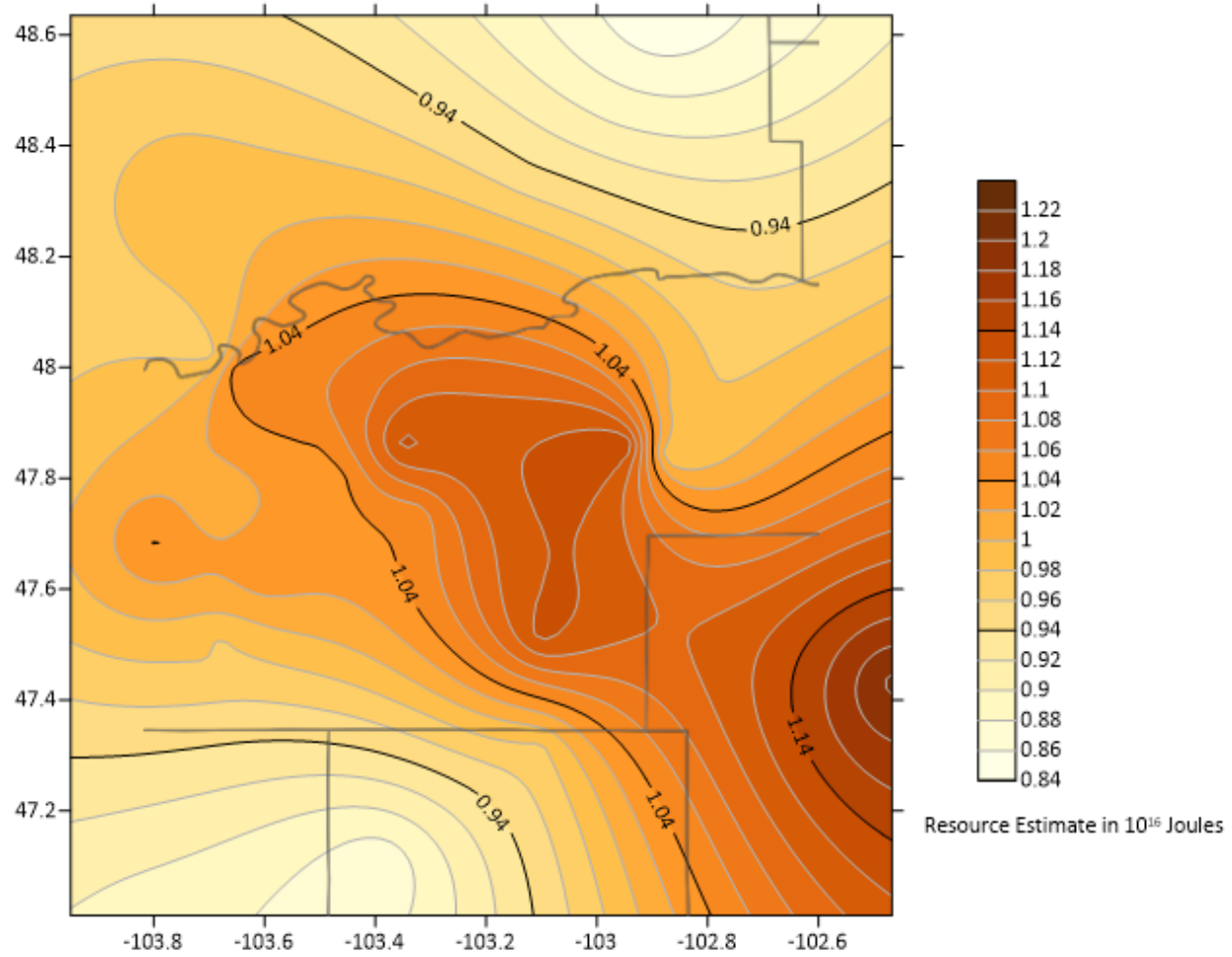


Figure 8 - Map showing resource estimates using the selected wells

4.5 Power Generation Estimation

Power generation potential was calculated using the following equation:

$$E = \rho C_v V(T_{\text{reservoir}} - 15^{\circ}\text{C}) \quad (10)$$

E is the power generated, ρ is the density of water (1030 kg m^{-3}), C_v is the heat capacity of water ($4181 \text{ J kg}^{-1} \text{ K}^{-1}$), V is the average volume of produced water ($\text{m}^3 \text{ h}^{-1}$), and ΔT is the change in temperature. This study assumed that the fluid temperatures at the wellhead were equal to the corresponding reservoir temperatures. However, power generated may vary based on whether the fluid has a significant temperature loss en route to the surface.

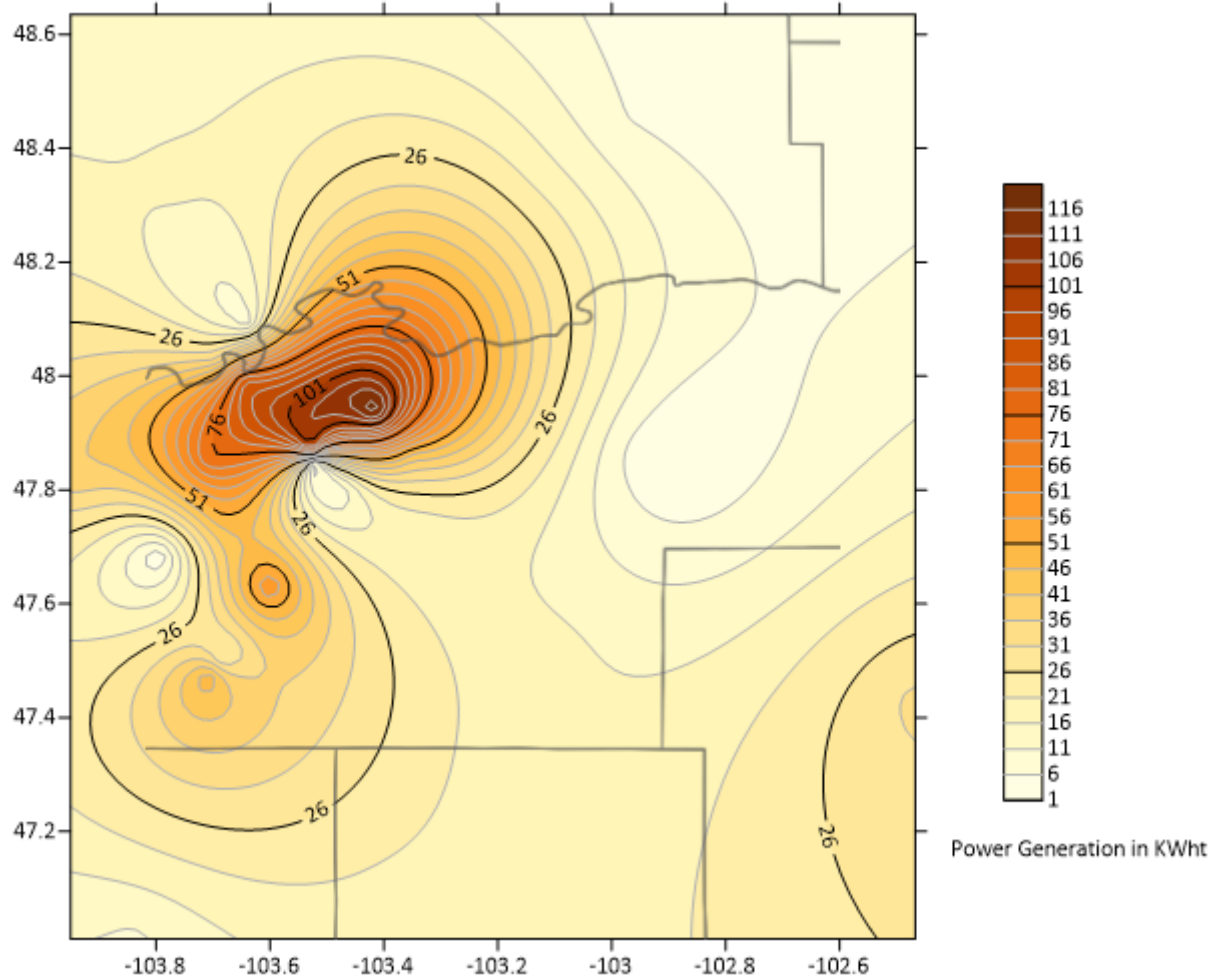


Figure 9 - Map showing the power generation potentials of the selected wells

5. DISCUSSION

This research study used oil and gas wells data from the NDIC database to investigate the factors determining site selection for geothermal energy extraction. The factors considered in this study included reservoir temperature, aquifer thickness, reservoir porosity, reservoir permeability, resource estimates, power generation estimates, and repurposing of abandoned wells to reduce drilling costs. The data from the NDIC database provided the bottom hole temperatures used to plot an estimated heat map using the Surfer software. The heat map (figure 5) identifies regions with a high potential heat source for geothermal extraction. This preliminary map showed that the Williston Basin covering most of the western part of North Dakota has more heat source potentials. Hence it was selected for a more focused evaluation.

The study investigated the aquifers underlying the Williston Basin. There are four principal aquifers, namely, Inyan Kara, Madison, Duperow, and Red River. An additional Formation called the Broom Creek was included in the aquifer assessment because of its lithology, porosity, and permeability. As the Red River Formation is the deepest of all the five Formations mentioned above, oil and gas wells deep into the Red River Formation were selected for the study. Another criterion in selecting the wells was that vertical wells were needed to calculate the temperature gradients accurately. Hence all the 28 wells used for the study were vertical (Figure 6). Figure 7 shows the map of temperature gradients. The pattern shown in the map indicates that the temperature increases westward of North Dakota.

Following the gradient mapping, the mean accessible resource was calculated for all five aquifers. This step was done to determine the size of the accessible energy resource in each region where wells are located. Resource estimates were calculated by applying the 25% recoverable factor. The mapping of the resource estimates using the Surfer software created a ranking system that delineates each category. Figure 8 shows that south of Williams County, north and east of McKenzie County, north-east Billings County, and West of Dunn County have the highest resource estimations.

Power generation capacity is a function of permeability, the volume of produced water, and temperature. The power generation estimates were done to add another ranking tool in selecting zones with a high potential of generating geothermal energy by considering the permeability of the reservoir. The study used a 6-month average of water production from each of the twenty-eight wells to calculate the

power generation potentials of the areas around those wells. Figure 9 shows that the northwest of McKenzie has the highest potential. There is a possibility that the high-power generation potential from the northwest of McKenzie County could be due to the recharge source from the Missouri River.

Recharge sources could play a role in site selection. For example, the Missouri River seems to be a decent recharge source in western North Dakota. Figure 10 shows that the river goes through several counties. Locations close to the river include south of Williams County, north and west of McKenzie County, south of Mountrail County, and north of Dunn County.

Another factor to consider in site selection for geothermal extraction is the cost of drilling. North Dakota has many wells on abandoned status. A total of 147 wells were placed on abandoned but not permanently abandoned at the time of this study. Out of the 147 wells, 93 wells are located in the counties identified with a high heat source for geothermal energy extraction. These counties are Williams, Mountrail, McKenzie, Dunn, Billings, and Golden Valley. These abandoned wells could be good candidates for retrofits into geothermal wells. Repurposing the abandoned wells into geothermal wells could be cost saving not for geothermal projects but for operators and North Dakota State in the permanent abandonment of wells.

Figure 10 shows the location of the 93 abandoned wells. The selection of the wells may depend on the total vertical depth, proximity of the wells to the selected favorable geothermal energy source sites.

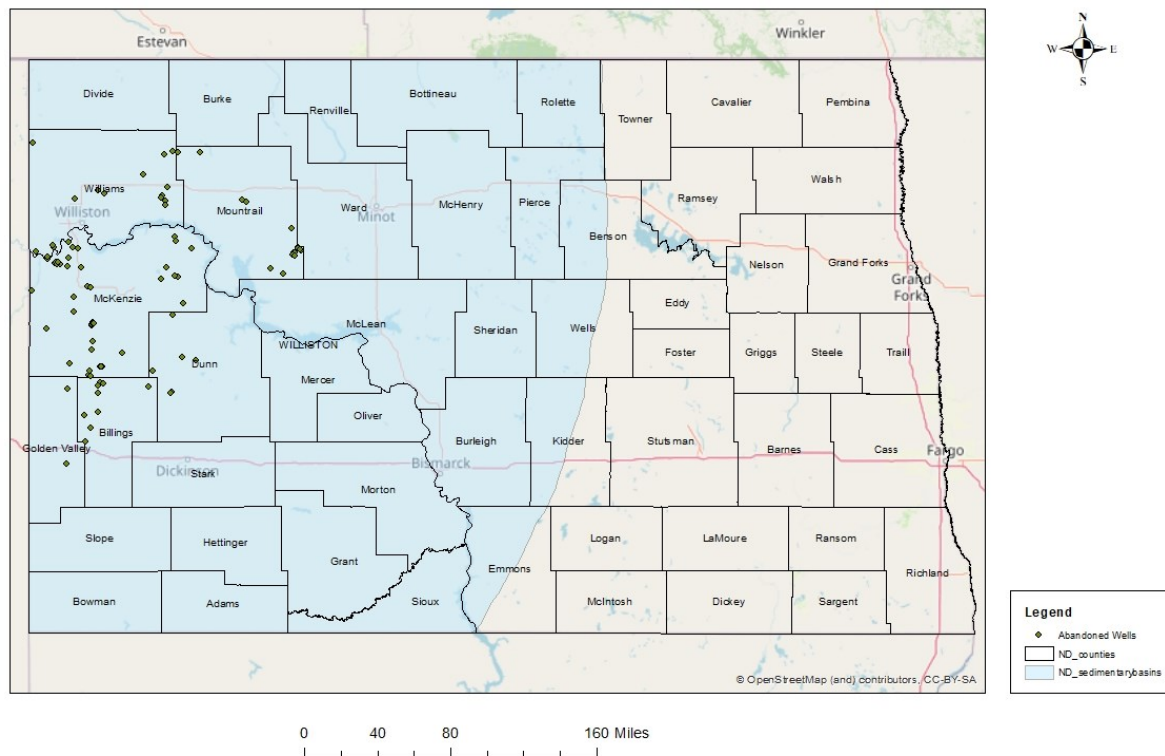


Figure 10 - Map showing abandoned wells in Williams, Mountrail, McKenzie, Dunn, Billings, and Golden Valley Counties

6. CONCLUSIONS

The results obtained in this study were grouped into three main parameters, namely, temperature gradient, resource estimation, and power generation potentials. The temperature gradient was calculated by using the calculated temperatures at depth. The resource estimation was calculated by applying a recoverable factor of 25% to the mean accessible resource formula. The mean accessible resource takes into consideration the thickness and specific heat capacity of the aquifers. Finally, the power generation potential considers the permeability of the reservoir, the temperature of the reservoir, and the volume of discharged water from a well.

In the model created to identify favorable locations for geothermal extraction, the results were ranked in the three main parameters. Then, these ranks were summed for individual wells. Next, the summed ranks (total) were ranked to obtain a combined rank (Table 6). All parameters were equally weighted for the sake of simplicity. The combined rank was finally used in creating the maps, as shown in Figures 11a, 11b, 11c, and 11d using the Surfer software. Site selection decisions could be made based on any or combined ranked results.

Table 6 - Summary of the results obtained from the study

File Number	Gradient (°C/km)	Resource Estimate (10 ¹⁶ Joules)	Power (KWh)	Rank	Gradient	Rank	Resource Estimate	Rank	KWh	Total	Combined Rank
9397	38.5	1.21	32.23	24.0		1.0		11.00	36.00	9.00	
8945	39.3	1.03	2.60	13.0		12.0		24.00	49.00	18.00	
18339	38.2	1.14	2.32	26.0		2.0		25.00	53.00	20.00	
15569	40.1	1.04	1.62	3.0		8.0		27.00	38.00	11.00	
11549	39.1	1.00	8.87	17.0		14.0		21.00	52.00	19.00	
12378	39.9	0.99	17.04	4.0		17.0		17.00	38.00	12.00	
9539	38.0	1.00	3.72	28.0		16.0		23.00	67.00	27.00	
15785	39.2	1.08	120.17	15.0		5.0		1.00	21.00	3.00	
9481	39.6	1.02	75.01	8.0		13.0		4.00	25.00	4.00	
15669	38.9	1.05	18.25	21.0		7.0		15.00	43.00	14.00	
15046	39.0	0.98	16.37	18.0		21.0		18.00	57.00	22.00	
15170	39.4	0.97	38.88	11.0		23.0		10.00	44.00	15.00	
7631	39.0	1.13	44.50	19.0		4.0		8.00	31.00	7.00	
16330	39.8	1.00	50.04	5.0		15.0		6.00	26.00	6.00	
7167	40.3	1.04	61.34	2.0		10.0		5.00	17.00	2.00	
16062	38.9	1.13	17.77	22.0		3.0		16.00	41.00	13.00	
6839	39.7	0.99	40.39	6.0		18.0		9.00	33.00	8.00	
22750	40.4	0.89	9.90	1.0		26.0		20.00	47.00	17.00	
12062	39.5	0.84	2.11	10.0		28.0		26.00	64.00	26.00	
11747	39.6	1.06	87.13	7.0		6.0		3.00	16.00	1.00	
16273	38.2	0.95	18.91	25.0		24.0		14.00	63.00	24.00	
12173	38.1	0.98	1.59	27.0		19.0		28.00	74.00	28.00	
12240	39.3	0.98	23.50	12.0		22.0		12.00	46.00	16.00	
12249	39.6	0.98	49.69	9.0		20.0		7.00	36.00	10.00	
11405	39.1	0.89	5.58	16.0		25.0		22.00	63.00	25.00	
9300	39.2	1.04	98.42	14.0		9.0		2.00	25.00	5.00	
17339	38.7	1.03	11.01	23.0		11.0		19.00	53.00	21.00	
15516	39.0	0.86	19.81	20.0		27.0		13.00	60.00	23.00	

Figures 11a, 11b, and 11c show the ranking of the thermal gradient, power generation potential, and resource estimate, respectively. Figure 11d shows the combined ranking model.

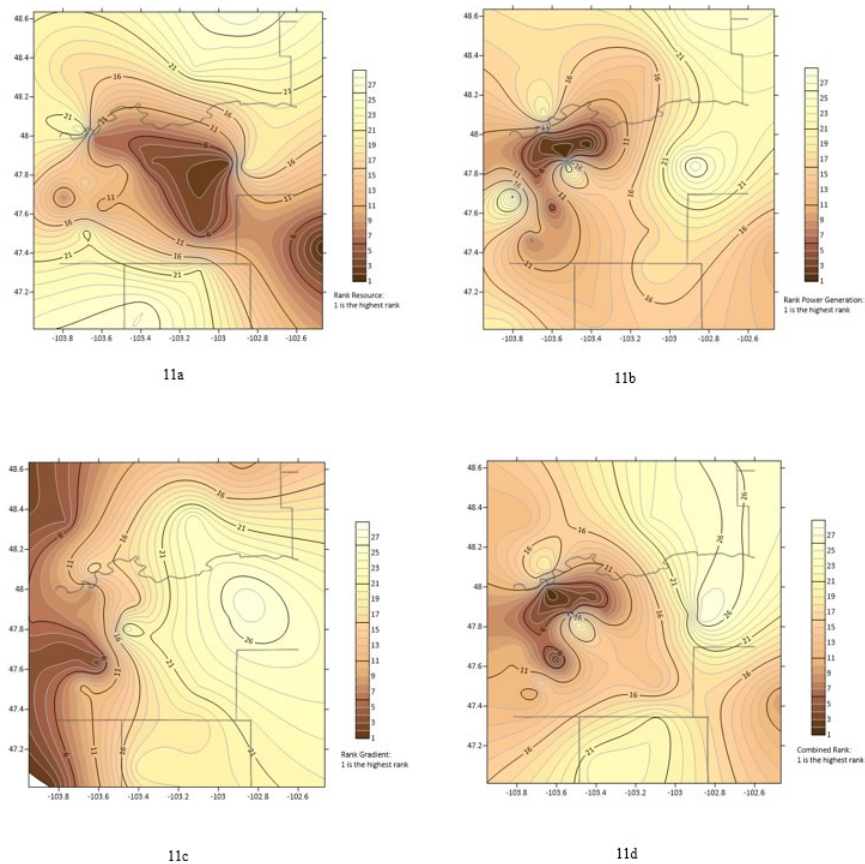


Figure 11 - Maps showing the ranking of the results obtained for resource estimates (11a), power generation (Figure 11b), temperature gradients (11c), and combined parameters (11d)

7. REFERENCES

Bader, J. (2017, January). *Mapping Sandstones of the Inyan Kara Formation for Saltwater Disposal in North Dakota*. <https://www.dmr.nd.gov/ndgs/documents/newsletter/2017Winter/Mapping%20Sandstones%20of%20the%20Inyan%20Kara%20Formation%20for%20Saltwater%20Disposal%20in%20North%20Dakota.pdf>

Beardsmore, G. R., & Cull, J. P. (2001). *Crustal Heat Flow*. Cambridge University Press.

Bertani, R. (2016). Geothermal power generation in the world 2010–2014 update report. *Geothermics*, 60, 31–43. [10.1016/j.geothermics.2015.11.003](https://doi.org/10.1016/j.geothermics.2015.11.003)

Downey, J. S., & Dinwiddie, G. A. (1988). *The regional aquifer system underlying the Northern Great Plains in parts of Montana, North Dakota, South Dakota, and Wyoming; summary*. [10.3133/pp1402a](https://doi.org/10.3133/pp1402a)

Erkan, K., Holdmann, G., Benoit, W., & Blackwell, D. (2008). Understanding the Chena Hot Springs, Alaska, geothermal system using temperature and pressure data from exploration boreholes. *Geothermics*, 37(6), 565–585. [10.1016/j.geothermics.2008.09.001](https://doi.org/10.1016/j.geothermics.2008.09.001)

Falcone, G., Liu, X., Okech, R. R., Seyidov, F., & Teodoriu, C. (2018). Assessment of deep geothermal energy exploitation methods: The need for novel single-well solutions. *Energy*, 160, 54–63. [10.1016/j.energy.2018.06.144](https://doi.org/10.1016/j.energy.2018.06.144)

Gosnold, W. D. Jr. (1991). *Stratabound geothermal resources in North Dakota and South Dakota*. [10.2172/6176983](https://doi.org/10.2172/6176983)

Gosnold, Will. (2021). *Power Generation Calculation for Geothermal Resources*. Heat Flow Class Lecture.

Gosnold, Will, Abudureyimu, S., Tsirypkin, I., Wang, D., & Ballesteros, M. (2019, June 17). *Geothermal and Electric Power Analysis of Horizontal Oil Well Fields Williston Basin, North Dakota, USA*. https://www.searchanddiscovery.com/documents/2019/80681gosnold/ndx_gosnold.pdf

Gosnold, Will, & Njoku, G. (2017). Heat Flow and Climate Change. GRC Transactions. <https://publications.mygeoenergynow.org/grc/1033846.pdf>

Gosnold, William, McDonald, M., Klenner, R., & Merriam, D. (2012). *Thermostratigraphy of the Williston Basin*. <http://citeserx.ist.psu.edu/viewdoc/download?doi=10.1.1.1065.644&rep=rep1&type=pdf>

Green, B., & Nix, G. (2006, November). *Geothermal—The Energy Under Our Feet*. NREL. <https://web.archive.org/web/20161228221939/http://www.nrel.gov/docs/fy07osti/40665.pdf>

Hartig, C. M. (2018). Porous media of the Red River Formation, Williston Basin, North Dakota: a possible Sedimentary Enhanced Geothermal System. *Int J Earth Sci (Geol Rundsch)*, 107(1), 103–112. [10.1007/s00531-016-1398-9](https://doi.org/10.1007/s00531-016-1398-9)

Ho, I.-H., Li, S., & Abudureyimu, S. (2019). Alternative hydronic pavement heating system using deep direct use of geothermal hot water. *Cold Regions Science and Technology*, 160, 194–208. [10.1016/j.coldregions.2019.01.014](https://doi.org/10.1016/j.coldregions.2019.01.014)

Jean Burrus (2), Kirk Osadetz (3),. (1996). A Two-Dimensional Regional Basin Model of Williston Basin Hydrocarbon Systems. *Bulletin*, 80. [10.1306/64ed87aa-1724-11d7-8645000102c1865d](https://doi.org/10.1306/64ed87aa-1724-11d7-8645000102c1865d)

LeFever, J. (2011, January). *The Spearfish Formation – Another Unconventional Target*. <https://www.dmr.nd.gov/ndgs/documents/newsletter/jan.2011/Jan2011Spearfish.pdf>

Liu, Y., Wang, G., Zhu, X., & Li, T. (2021). Occurrence of geothermal resources and prospects for exploration and development in China. *Energy Exploration & Exploitation*, 39(2), 536–552. [10.1177/0144598719895820](https://doi.org/10.1177/0144598719895820)

Majorowicz, J. A., Jones, F. W., & Osadetz, K. G. (1988, March). *Heat Flow Environment Of The Electrical Conductivity Anomalies In The Williston Basin, And Occurrence Of Hydrocarbons: GEOLOGICAL NOTE*. The AAPG/Datapages. <https://archives.datapages.com/data/cspg/data/036/036001/0086.htm>

Medium-Term Renewable Energy Market Report 2013. (2013). [10.1787/9789264191198-en](https://doi.org/10.1787/9789264191198-en)

Muffler, P., & Cataldi, R. (1977). *Methods for regional assessment of geothermal resources*. [10.2172/6496850](https://doi.org/10.2172/6496850)

Murphy, E., Nordeng, S., Juenger, B., & Hoganson, J. (2009). *North Dakota Stratigraphic Column*. North Dakota Geological Survey. [https://www.dmr.nd.gov/ndgs/documents/Publication_List/pdf/Strat-column-NDGS-\(2009\).pdf](https://www.dmr.nd.gov/ndgs/documents/Publication_List/pdf/Strat-column-NDGS-(2009).pdf)

ND State Water Commission Mapservices. (n.d.). Retrieved May 18, 2021, from https://www.swc.nd.gov/info_edu/map_data_resources/mapservices.html

NDIC Oil and Gas Division. (n.d.). *North Dakota Oil and Gas Division*. <https://www.dmr.nd.gov/oilgas/>

Nian, Y.-L., & Cheng, W.-L. (2018). Insights into geothermal utilization of abandoned oil and gas wells. *Renewable and Sustainable Energy Reviews*, 87, 44–60. [10.1016/j.rser.2018.02.004](https://doi.org/10.1016/j.rser.2018.02.004)

North Dakota Geologic Survey. (n.d.). *North Dakota Geothermal Maps*. <https://www.dmr.nd.gov/ndgs/geothermal/geothermalmaps.asp>

Peterson, J. A. (1984). *Stratigraphy and sedimentary facies of the Madison Limestone and associated rocks in parts of Montana, Nebraska, North Dakota, South Dakota, and Wyoming*. [10.3133/pp1273a](https://doi.org/10.3133/pp1273a)

Selley, R. C. (2014). *Elements of Petroleum Geology* (2nd ed.). Academic Press.

Smith, S. A., Beddoe, C. J., Mibeck, B. A. F., Heebink, L. V., Kurz, B. A., Peck, W. D., & Jin, L. (2017). Relative Permeability of Williston Basin CO₂ Storage Targets. *Energy Procedia*, 114, 2957–2971. [10.1016/j.egypro.2017.03.1425](https://doi.org/10.1016/j.egypro.2017.03.1425)

Obinwa

Sorey, M., Reed, M., Foley, D., & Renner, J. (1970, January 1). *Low-Temperature Geothermal Resources in the Central and Eastern United States, Assessment Of Low-temperature Geothermal Resources Of The United States - 1982 (Technical Report)* | OSTI.GOV (M. Reed, Ed.). <https://pubs.usgs.gov/circ/1983/0892/report.pdf>

Sowa-Watrak, A., Klosok-Bazan, I., Gono, M., & Gono, R. (2017, May 1). *The Criteria For Suitable Location Of Geothermal Power Plant*. ResearchGate. https://www.researchgate.net/publication/318327298_The_criteria_for_suitable_location_of_geothermal_power_plant

State Of North Dakota Water Feature Map And List Of County Lakes, Rivers, Streams - CCCarto. (n.d.). Retrieved June 7, 2021, from <https://www.cccarto.com/statewaters/northdakota/>